ELSEVIER

4 September 1995

PHYSICS LETTERS A

Physics Letters A 205 (1995) 18–24

Controlling chaos to store information in delay-differential equations

Boualem Mensour [1], André Longtin [2,*]

Département de Physique, Université d'Ottawa, 150 Louis Pasteur, Ottawa, Ontario, Canada K1N 6N5

Received 2 March 1995; revised manuscript received 19 July 1995; accepted for publication 20 July 1995
Communicated by C.R. Doering

Abstract

The Mackey–Glass delay-differential equation exhibits multistability when the ratio of delay to response time is large. A piecewise constant initial function corresponding to a finite message can then be stored into a periodic waveform. We show that the storage capability is enhanced by the control of unstable periodic orbits in the chaotic regime. Further, the relative controllability of these orbits is quantified using a low-dimensional discrete-time map obtained in a singular limit of this system.

Keywords: delay-differential equations; control; chaos; multistability; memory; difference equations; information storage; feedback

1. Introduction

First-order nonlinear delay-differential equations (DDEs) are infinite-dimensional dynamical systems. They evolve forward in time from an initial function defined over one delay interval. The Mackey–Glass and the Ikeda equations [1], which belong to this class of dynamical systems and which are of interest here, model the rate of change of the state variable as a balance between an instantaneous linear response and a delayed nonlinear feedback (see Eq. (1) below). When the feedback delay is much greater than the response time of the system, the dynamics exhibit multistability [2,3]. This means that, while a given initial function uniquely specifies the solution, the functional space in which these equations evolve has more than one basin of attraction. Hence, the asymptotic solution depends on the choice of initial function.

This multistability in the time domain makes systems modeled by such equations attractive for memory storage purposes, an idea first suggested by Ikeda and Matsumoto [3]. This strategy has recently been implemented on a hybrid laser diode modeled by the Ikeda equation [4]. A message, in the form of a finite sequence of binary numbers, specifies the successive values of plateaus in a piecewise constant initial function for the system. When the delay is sufficiently large, the system evolves in time into a periodic waveform uniquely specified by this sequence. A requirement of this technique is that the system parameters, namely those controlling the strength of the feedback, be chosen such that the dynamics exhibit stable periodic behavior.

The dynamics of these systems become chaotic when e.g. the strength of the feedback is increased

* Corresponding author.
[1] E-mail: boualem@physics.uottawa.ca.
[2] E-mail: andre@physics.uottawa.ca.

Elsevier Science B.V.
SSDI 0375-9601(95)00555-2

[1]. However, the exponential divergence of trajectories does not allow the memory storage strategy to work in the chaotic regime. While multistability still exists in this regime at large delay, even the memory of a constant initial function is lost in the chaotic evolution, as shown in Fig. 1a for the Mackey–Glass equation. In the chaotic regime, an infinite number of unstable periodic orbits (UPOs) coexist with one or more chaotic attractors [2,3]. These periodic solutions are not visible for typical initial conditions, although chaotic trajectories can spend time near them before being repelled away.

In this Letter, we show that unstable periodic orbits of the Mackey–Glass equation can be observed using a recently proposed chaos control technique [5], and more importantly, that memory storage is also possible in these controlled waveforms. We find that the chaotic regime allows for an enhanced versatility of memory storage since, for fixed parameters in the uncontrolled system, UPOs of different periods can be controlled by tuning one control parameter. Further, we present a theoretical analysis of the controllability of the UPOs in such infinite-dimensional dynamical systems using a low-dimensional discrete-time map. This map arises in the singular limit of the DDE in which the delay to response time ratio R goes to infinity. The controllability is found to be predictable by the Lyapunov exponents and other characteristics of this map.

The control of UPOs in other high-dimensional systems such as partial differential equations [6] has been reported. The large number of UPOs and the sensitivity to small perturbations endow chaotic systems with a flexibility to produce different patterns using minimal perturbations and without changing system parameters [7]. Our method benefits from this flexibility. There have also been recent studies of chaos in the context of message encryption and transmission, as in a seminal paper [8] where this is achieved using the synchronization of chaotic systems. Also, Hayes et al. [9] have shown that the oscillations of a chaotic system can be made to follow, using small perturbations, a desired sequence of symbols, thus encoding an arbitrarily long message into a waveform. In contrast, our method involves the storage of finite messages. However, it relies on multistability rather than on the system's symbolic dynamics which preclude certain symbol sequences. Consequently, in our method, messages are directly encodable without the necessity of a "grammar" as in Ref. [9]. Our results provide insight into multistability in simple DDE models of neural feedback [10] and in control systems, physiological and other, involving multiple delayed feedback loops [11]. Our method further provides an alternative to models of temporal pattern storage based on networks of many coupled neurons [12].

2. Solutions of the Mackey–Glass equation at large delays

Our study focusses on numerical simulations of the Mackey–Glass equation

$$\frac{\mathrm{d}x(t)}{\mathrm{d}t} = -bx(t) + \frac{ax(t-\tau)}{1+x^c(t-\tau)}. \tag{1}$$

With parameters (constant throughout our study) $a = 0.145, b = 0.1, c = 10$, Eq. (1) exhibits aperiodic behavior when the delay time $\tau > 42$ (see Fig. 1a). Although we have not analyzed this motion in detail using e.g. dimension or Lyapunov spectrum calculations, this aperiodicity is consistent with earlier reports of deterministic chaos in this parameter range [1,13]; the behavior is thus assumed to be chaotic. The multistability of this DDE is easily characterized (see e.g. Ref. [4]) when (i) the parameters yield a stable periodic solution (e.g. for $a < 0.14$) and (ii) the feedback delay τ is much greater than the system response time $t_r = b^{-1}$. The initial functions of interest here are piecewise constant, each constant corresponding to a binary number in a code. The continuous solution then consists of "plateaus" linked together by short transitions of width proportional to $2t_r/\tau$ [14]. The solution ressembles that in Fig. 1b (which however is a controlled UPO), without the small spikes at the end of the plateaus. Each plateau evolves from its initial constant independently from the other plateaus. After transients, all plateaus cycle through the same set of values in the same order. In the singular limit $R \equiv \tau/t_r \to \infty$ of the DDE, these values are exactly given by the asymptotic solution of the difference equation

$$x(t) = b^{-1} f(x(t-\tau)) = \frac{b^{-1}ax(t-\tau)}{1+x^c(t-\tau)}. \tag{2}$$

Such an equation has previously been used to study properties of DDEs like stability and bifurcations [14]

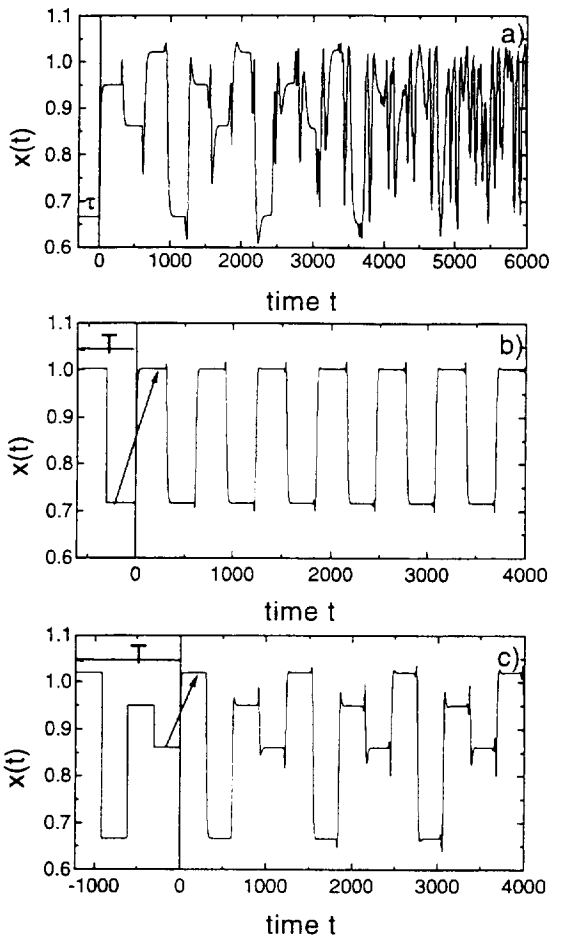

Fig. 1. Numerical solutions of Eq. (1) for a ratio of delay to system response time $R = 30$. Other parameters are $\tau = 300$, $a = 0.145$, $b = 0.1$ and $c = 10$. (a) Chaotic regime. The constant initial function on $(-\tau, 0)$ evolves into a solution whose plateaus shrink and finally disappear, leaving no trace of this initial condition. (b) A second feedback term with delay T (see Eq. (3)) is used to stabilize the unstable periodic orbit P_1 (see text). The initial function is a constant on $(-T, 0)$. The solution oscillates between two values determined by Eq. (4), and reflects the value of the initial function. The control parameters are $K = 0.05$ and $T = 616.4$. (c) Same as in (b) but $T = 1225.4$. This allows the control of the unstable periodic orbit P_2 which cycles between four values determined by Eq. (4).

and the influence of noise [15]. One can go one step further and discretize the continuous time in Eq. (2) in units of τ. The evolution of each point on $(-\tau, 0)$ is then governed by the one-dimensional map $x(i) = b^{-1} f(x(i-1))$. All points on $(-\tau, 0)$ are mapped in parallel from one delay interval to the next. These points evolve independently since, in this limit, the solution is not constrained to be continuous. Eq. (2) is of course multistable, except when the singular limit map has one globally attracting fixed point (which occurs at much lower values of a). For values of R on the order of 30, as in our study, Eq. (2) adequately predicts the plateau values for periodic solutions.

3. Controlling unstable periodic orbits at large delays

Unstable periodic orbits in Eq. (1) are controlled using a delayed negative feedback of the form $F(t) \equiv K[x(t-T) - x(t)]$ following the method of Ref. [5] for ordinary differential equations. T is the period of the selected UPO and K is the control parameter. The dynamics then become

$$\frac{dx(t)}{dt} = -bx(t) + f(x(t-\tau)) + K[x(t-T) - x(t)] . \quad (3)$$

For a piecewise constant initial function, the plateaus in the solution of Eq. (3) cycle through values approximately given by the orbits of the difference equation obtained in the singular limit ($R \to \infty$) of Eq. (3),

$$x(t) = \frac{1}{b+K}[f(x(t-\tau)) + Kx(t-T)] . \quad (4)$$

Note that this is a continuous-time difference equation like Eq. (2). Fig. 2a illustrates this stable periodic orbit on the discrete time map associated with Eq. (2), to avoid the three-dimensional representation using the variables $x(t)$, $x(t-\tau)$ and $x(t-T)$ from Eq. (4). The period-four orbit in Fig. 2a is unstable without the second delayed feedback, since without this term the dynamics are chaotic with $a = 0.145$. Fig. 2b shows the solution of Eq. (4) corresponding to the "stabilized" period-four orbit in Fig. 2a. The perturbation $F(t)$ is small when the trajectory lies close to an UPO of the uncontrolled system. We focus here on these UPOs rather than on new orbits created by the control. This second delayed feedback can be switched on at any time; control occurs after transients have died out.

We have found that a plot of the limit cycle amplitude versus τ for Eq. (3) can be used to estimate the maximum number of plateaus, in one delay τ, which

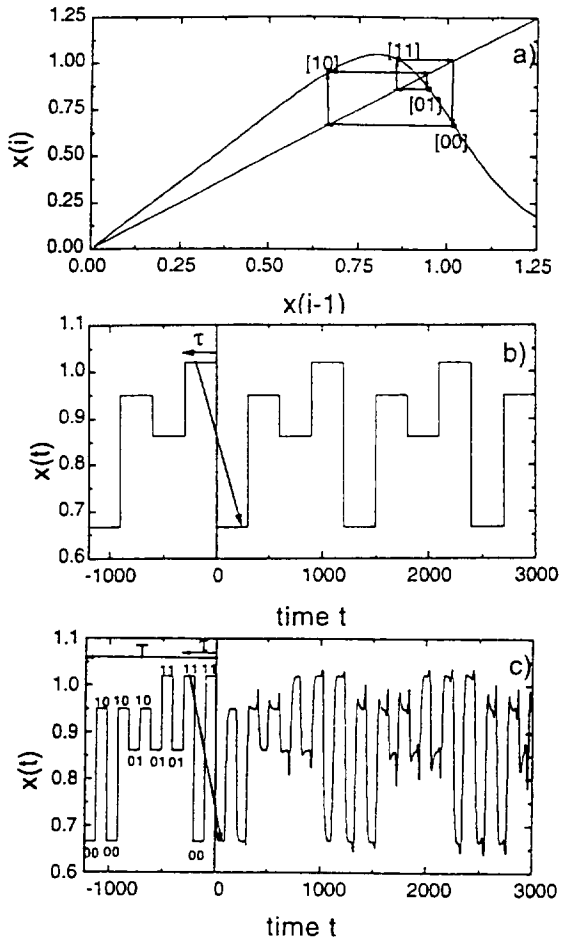

Fig. 2. Storage of a finite message into the controlled periodic waveform P_2 with $K = 0.05$. (a) Discrete-time map $x(i) = b^{-1}f(x(i-1))$ obtained by letting $R \to \infty$ in Eq. (1) to obtain Eq. (2), and discretizing time in units of τ. Without control, this map has an unstable period-four orbit (shown on the map), cycling through [11], [01], [10], [00]. With control ($T = 4\tau = 1200$) this same period-four orbit, governed by Eq. (6), is stable. (b) Solution of the difference equation Eq. (4) obtained in the singular limit of Eq. (3), with $T = 4\tau$. The initial function on $(-T, 0)$ is chosen to be piecewise constant, with constants equal to one of the four values of the controlled period-four orbit in (a). This periodic waveform has period T. (c) Storing the sequence [11,00,11] within a delay τ into the solution of the controlled delay-differential equation (Eq. (3)). The control delay is $T = 1225.4$, which is also the period of the waveform, close to the value of $4\tau = 1200$ in (b). To minimize transients, the plateaus on $(-T, -\tau)$ were chosen such that the perturbation $F(t) = K|x(t-T) - x(t)|$ is close to zero. This is achieved by choosing these plateaus as the three pre-images, dictated by the map in (a), of the message on $(-\tau, 0)$.

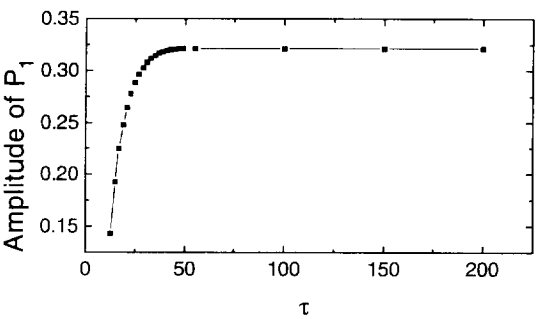

Fig. 3. Amplitude of the limit cycle of the controlled delay-differential equation (3) as a function of τ. A Hopf bifurcation occurs at $\tau = 11.2$.

can evolve in time without merging. For the parameters chosen, a Hopf bifurcation occurs at $\tau = 11.2$, and for $\tau > \tau_c \approx 43$ this amplitude saturates, as shown in Fig. 3. The approximate number of plateaus is found to be $\tau/\tau_c \approx 7$ since $\tau = 300$ in our study. This holds over the wide range of K values for which this limit cycle can be controlled (without control, the first period-doubling occurs at $\tau = 28.1$). If an initial function with more than seven plateaus is used, the transition time between plateaus becomes comparable with the width of one plateau, and merging occurs.

A desired UPO can be stabilized by substituting either the fixed point x^* or $x(t-\tau)$ for $x(t-T)$ in Eq. (3). The linear stability analysis of the map in the singular limit of Eq. (3) (see Eq. (4), or Eq. (6) below) shows that the fixed point is stable for $K > -[f'(x^*) + b]$ in the first case, and if $K > -[f'(x^*) + b]/2$ in the second. If K is smaller than these values, it is possible to control period-doubled solutions, which have more states and thus are more interesting for memory storage. Our discussion will focus on controlling P_1, the limit cycle arising through a Hopf bifurcation, and P_2, its first period-doubled solution. Note that in the singular limit, the Hopf bifurcation becomes the first period-doubling bifurcation of the map [14,15]. Substituting x^* or $x(t-\tau)$ for $x(t-T)$, one observes a solution with approximately the right period, but the wrong amplitude. This measured period is very close to that of the desired UPO; it can then be used for T in Eq. (3) to properly control the UPO. For P_1 and P_2, a fine-tuning as in Figs. 4a and 4b will further decrease $F(t)$ until P_1 or P_2 are optimally controlled. For constant R, the range of

controllability of P_2 is much narrower than that for P_1. Higher P_N are increasingly difficult to control. The resulting controlled P_2 is shown in Fig. 1c. This method enabled us to also control UPOs in the Ikeda equation.

4. Storing finite messages using piecewise constant initial functions.

We now show how a sequence of binary numbers can be encoded into one of the many possible waveforms of an UPO of a given period. Again, this multistability in Eq. (3) arises because the delay is large. Following Ref. [4], we define a "(n,l) isomer" as a solution with n plateaus in one delay τ, each cycling through the l values of P_N. There are l^n different initial functions or "messages" which can be stored. The maximum storage capacity is achieved when the initial function has the maximum number of plateaus that can evolve without merging; it is given by l^{τ/τ_c}. A binary number can be assigned to each of the l values, in a ranked fashion with the lowest binary number corresponding to the lowest of the l values. The number of bits for each value is given by $\log_2(l)$. For example, P_2 cycles through four values; thus, a two-bit code can be assigned to each of the four values: 00, 01, 10, or 11.

The controlled singular limit map obtained by discretizing time in units of τ in Eq. (3) is given by

$$x(i) = b^{-1} f(x(i-1)) + b^{-1} K[x(i-l) - x(i)], \tag{5}$$

which can be rewritten as

$$x(i) = \frac{1}{b+K}\left[f(x(i-1)) + Kx(i-l)\right]. \tag{6}$$

For a certain range of K, an orbit of period l can be controlled. As the perturbation $K[x(i-l) - x(i)]$ in Eq. (5) vanishes when the control is achieved, the orbit cycles between l points on the map $x(i) = b^{-1} f(x(i-1))$. If, for example, $K = 0$, this map is chaotic; however, if $K = 0.05$, a controlled P_2 orbit cycling between four values is obtained, as shown in Fig. 2a. An $(n = 3, l = 4)$ isomer for the DDE carrying the information [11,00,11] in a solution of period 1225.4 (which is approximately $l\tau = 4\tau = 1200$) is shown in Fig. 2c. The map in Eq. (5) accurately predicts the evolution of the mean values of the plateaus

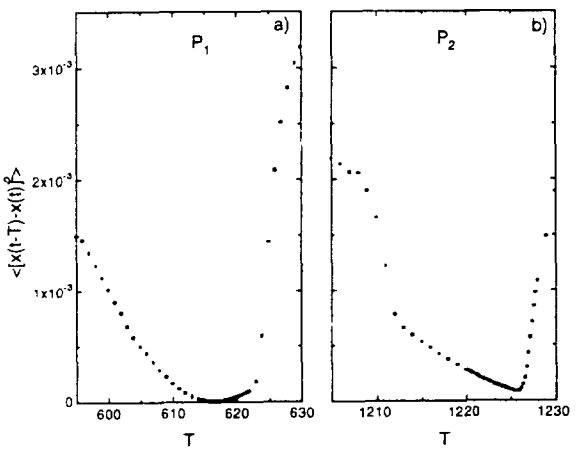

Fig. 4. Plot of the dependence of the dispersion $\langle [x(t-T) - x(t)]^2 \rangle$ on the delay T of the second feedback loop in Eq. (3) with $K = 0.05$ and $\tau = 300$. The quality of the control is inversely proportional to this dispersion. (a) P_1 with $T = 616.4$; (b) P_2 with $T = 1225.4$.

for this DDE. Comparing Fig. 2c to the singular limit case in Fig. 2b, one sees small spikes near the transition points, which the control cannot eliminate. Nevertheless, this waveform is stable and preserves the memory of the initial function.

5. Stability and controllability of orbits

The map (6) can also be used to assess the range of K values for which a desired UPO can be controlled. Fig. 5a plots the dispersion $\langle |x(t-T) - x(t)| \rangle$ (similar to the dispersion in Fig. 4) versus K for the DDE and for Eq. (4), its associated difference equation. For Eq. (4), this dispersion is zero when control is achieved. Fig. 5a shows that the difference equation approximation of the DDE is justified, even for $R = 30$, since both dispersions have a similar dependence on K over the range of K where P_2 is controllable.

The Lyapunov exponents for Eq. (6) can also be used to study the stability of the orbits. This l-dimensional map is first converted into l coupled one-dimensional maps,

$$y_0(i) = \frac{1}{b+K}[f(y_0(i-1)) + Ky_1(i-1)],$$

$$y_j(i) = y_{j+1}(i-1), \quad j = 1, 2, \ldots, l-2,$$

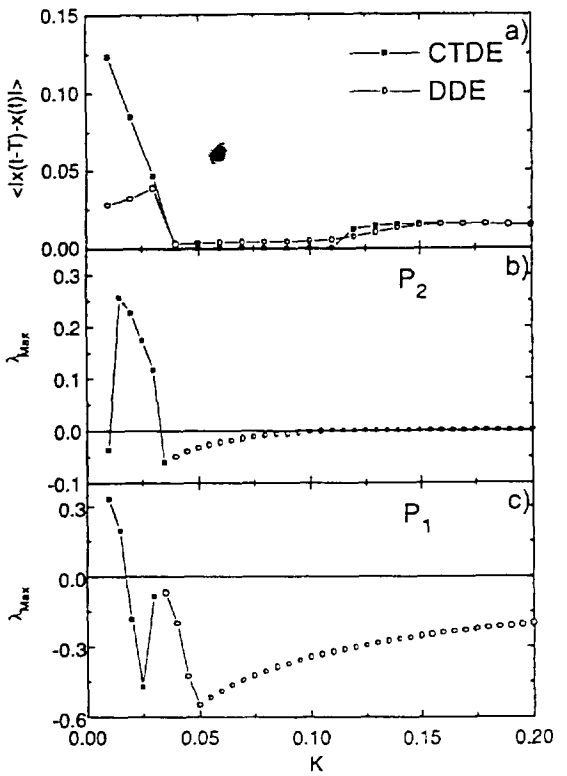

Fig. 5. Investigating the controllability of UPOs as a function of the control parameter K. (a) Dispersion $\langle |x(t-T)-x(t)| \rangle$ of P_2 for the continuous-time difference equation (4) (CTDE) and for the delay–differential equation (3) (DDE). (b) Maximal Lyapunov exponent of the map (6) for P_2. (c) Same as in (b) but for P_1. The filled squares at low K with $\lambda_{\mathrm{Max}} < 0$ in (b) and (c) correspond to other orbits of higher period.

$$y_{l-1}(i) = y_0(i-1). \tag{7}$$

The Lyapunov exponents are then calculated using the QR decomposition method [16] in the implementation of Ref. [17]. Figs. 5b and 5c show the maximum Lyapunov exponent λ_{Max} for, respectively, P_2 and P_1 as a function of K. Comparing the regions where $\lambda_{\mathrm{Max}} < 0$, we see that P_1 has a larger range of stability than P_2. The K-range for P_2 decreases when a in Eq. (3) increases until it vanishes for $a > 0.151$ and we are unable to control this orbit (not shown). However if we then increase K, control can be achieved but for a limited time only, as λ_{Max} is close to zero. Finally, good agreement is found between the stability domains based on the dispersion $\langle |x(t-T)-x(t)| \rangle$ and λ_{Max}. Fig. 5 clearly indicates that P_2 is stable only in the range $K \in [0.04, 0.11]$, while P_1 is stable for any value of $K > 0.035$.

6. Conclusion

We have shown that the multistability of controlled unstable periodic orbits of the Mackey–Glass delay–differential equation at large delay can be exploited to store finite messages into periodic waveforms. As our method is based on the chaotic rather than periodic regime, a broader range of waveforms of different shapes and periods can be accessed by tuning the control delay. Our analysis shows that the properties of this high-dimensional dynamical system, and in particular, the controllability of its UPOs (as measured by the maximal Lyapunov exponent and the dispersion), can be predicted by a low-dimensional map obtained in a singular limit of this DDE. Increasing the ratio of delay to response time in the uncontrolled system allows isomers of increasing complexity to be controlled. We have found (not shown) that a moderate-to-high noise level increases the amplitude of the perturbation $F(t)$; this can cause the solution to jump from one basin of attraction to another, and thus degradation of the memory. However, a small amount of noise merely adds a bit of structure on the plateaus, without altering the basic period and message content of the waveform.

Acknowledgement

This research was supported by NSERC Canada as well as by a CIDA fellowship to BM. The authors thank John Milton for useful discussions.

References

[1] M.C. Mackey and L. Glass, Science 197 (1977) 287;
K. Ikeda, H. Daido and O. Akimoto, Phys. Rev. Lett. 45 (1980) 709.

[2] K. Ikeda, K. Kondo and O. Akimoto, Phys. Rev. Lett. 49 (1982) 1467;
J.N. Li and B.L. Hao, Commun. Theor. Phys. 11 (1989) 265;
J. Losson, M.C. Mackey and A. Longtin, Chaos 3 (1993) 167.

[3] K. Ikeda and K. Matsumoto, Physica D 29 (1987) 223.

[4] T. Aida and P. Davis, IEEE J. Quantum Electron. 28 (1992) 686.
[5] K. Pyragas, Phys. Lett. A 170 (1992) 421.
[6] H. Gang and H. Kaifen, Phys. Rev. Lett. 71 (1993) 3794.
[7] T. Shinbrot, C. Grebogi, E. Ott and J. Yorke, Nature 363 (1993) 411.
[8] L.M. Pecora and T.L. Carroll, Phys. Rev. Lett. 64 (1990) 821;
K.M. Cuomo and A.V. Oppenheim, Phys. Rev. Lett. 71 (1993) 65.
[9] S. Hayes, C. Grebogi and E. Ott, Phys. Rev. Lett. 70 (1993) 3031.
[10] R.E. Plant, SIAM J. Appl. Math. 40 (1) (1981) 150;
M.C. Mackey and U. an der Heiden, J. Math. Biology 19 (1984) 211;
J.G. Milton, U. an der Heiden, A. Longtin and M.C. Mackey, Biomed. Biochem. Acta 49 (1990) 697.
[11] L. Glass and C.P. Malta, J. Theor. Biol. 145 (1990) 217;
J.G. Milton, S.A. Campbell and J. Bélair, J. Biol. Syst. (1995), to be published.
[12] D. Kleinfeld, Proc. Nat. Acad. Sci. USA 83 (1984) 9469;
H. Sompolinsky and I. Kanter, Phys. Rev. Lett. 57 (1986) 2862;
C.M. Marcus and R.M. Westervelt, Phys. Rev. A 39 (1989) 347;
A.V.M. Herz, Phys. Rev. A 44 (1991) 1415.
[13] J.D. Farmer, Physica D 4 (1982) 366.
[14] S.N. Chow and J. Mallet-Paret, in: Coupled nonlinear oscillators, eds. J. Chandra and A.C. Scott (North-Holland, Amsterdam, 1983);
J. Mallet-Paret and R.D. Nussbaum, in: Chaotic dynamics and fractals, eds. M.F. Barnsley and S.G. Demko (Academic Press, New York, 1986).
[15] A. Longtin, Phys. Rev. A 44 (1991) 4801.
[16] J.P. Eckmann and D. Ruelle, Rev. Mod. Phys. 57 (1985) 617.
[17] H.D.I. Abarbanel, R. Brown and M.B. Kennel, J. Nonlinear Sci. 2 (1992) 343.